



Synthesis and Tribological Properties of Zeolitic Imidazolate Framework-8 Nanocrystals and Microcrystals

WEI-CHAO SUN, QI SHI*, HONG XU and JIN-XIANG DONG*

Research Institute of Special Chemicals, Taiyuan University of Technology, Taiyuan 030024, Shanxi Province, P.R. China

*Corresponding authors: Fax: +86 351 6111178; Tel: +86 351 6010550; E-mail: shiqi594@163.com; dongjinxiangwork@hotmail.com

Received: 16 November 2013;

Accepted: 14 February 2014;

Published online: 26 December 2014;

AJC-16511

The nano- and microcrystalline zeolitic imidazolate framework-8 (ZIF-8) were synthesized using two different methods and had average diameters of approximately 100 nm and 1-10 μm , respectively. The tribological properties of ZIF-8 nano- and microcrystals as additives in a base oil (PEG200) were evaluated using a four-ball tester. Both products exhibited good friction behavior when used as additives in PEG200. In particular, when 0.5 wt. % nanocrystalline or microcrystalline ZIF-8 was added to PEG200, the tribological properties of the oil improved: its maximum nonseizure load (P_B) increased by 7.60 and 17.25 % for the nanocrystalline and microcrystalline ZIF-8, respectively; and its wear scar diameters (WSD) decreased by 31.35 and 30.76 %, respectively.

Keywords: Nanostructures, Microstructure, Tribology, Wear.

INTRODUCTION

Zeolitic imidazolate frameworks (ZIFs) are a new, distinctive and rapidly developing subclass of metal-organic frameworks. Due to their attractive features such as large surface areas and high thermal and chemical stability¹, ZIFs have become promising candidate materials for many technological applications such as gas adsorption², separation^{2,3}, catalysis⁴ and so on. Cheetham *et al.*⁵ reported that ZIF-8 (the most typical ZIF) has a remarkably low shear modulus that may reduce friction at interfaces. Our group reported that ZIF-8 used as additives in 100 SN oil lubricants show good antiwear and load-carrying properties⁶.

Generally, the properties and performance of the materials are highly dependent on the size of the crystal particles^{7,8}. In tribology, some nanomaterials have been proved to have great potential as lubricating materials⁹. Therefore, it is of significance to study the different particle sizes of ZIF-8 as lubricating oil additives and discover what effects will occur under friction in order to gain a better understanding of the tribological mechanism of ZIF-8 and thereby put the synthesis of ZIF-8 on a more rational basis. In this paper, identical solvents were chosen in order to synthesize ZIF-8 nano- and microcrystals.

The physical characteristics of ZIF-8 nano- and microcrystals are characterized and their tribological properties are evaluated under the same conditions by using a four-ball test. Powder X-ray diffraction (PXRD), scanning electron microscopy (SEM) and energy dispersive X-ray spectroscopy (EDS)

analyses were carried out to determine the possible lubrication mechanism of these nano- and microcrystals.

EXPERIMENTAL

2-Methylimidazole (MIM, 99 %), zinc nitrate hexahydrate [$\text{Zn}(\text{NO}_3)_2 \cdot 6\text{H}_2\text{O}$, 98 %] and zinc acetate dihydrate [$\text{Zn}(\text{OAc})_2 \cdot 2\text{H}_2\text{O}$, 98 %] were purchased from Sigma-Aldrich Chemical Co. Methanol (CH_3OH , 99.5 %) and polyethylene glycol 200 (PEG 200, with a viscosity index of 22.3) were obtained from Sinopharm Group Chemical Reagent Co. Petroleum ether were purchased from Aladdin industrial corporation. All raw chemicals were used without further purification.

Synthesis of ZIF-8 nanocrystals: Three grams (10.08 mmol) of $\text{Zn}(\text{NO}_3)_2 \cdot 6\text{H}_2\text{O}$ were dissolved in 200 mL of MeOH. A second solution was prepared by dissolving 3.28 g (39.95 mmol) of 2-methylimidazole in 200 mL of MeOH. The latter clear solution was poured into the former clear solution and they were stirred together at room temperature for 24 h¹⁰. The crystals were then centrifuged with speeds 9000 rpm (150 s^{-1}) by using centrifuge TG16-WS (Hunan Xiangyi Laboratory Instrument Development Co. Ltd), washed ultrasonically with ethanol and dried in air.

Synthesis of ZIF-8 microcrystals: $\text{Zn}(\text{OAc})_2 \cdot 2\text{H}_2\text{O}$ (1.76 g, 8.02 mmol), 2-methylimidazole (1.97 g, 23.99 mmol) and an MeOH solution (100 mL) were mixed in a Teflon-lined autoclave and stirred for 15 min. The autoclave was then sealed and heated at 100 °C for 3 days, followed by cooling to the

room temperature. Aggregated particles were firstly centrifuged and removed with speeds 300 rpm (5 s^{-1}), and the crystals were then centrifuged with speeds 3000 rpm (50 s^{-1}), washed ultrasonically with ethanol and dried in air.

Friction and wear tests: The ZIF-8 nano- and microcrystals were separately added to PEG 200 at concentrations of 1.0, 2.0 and 3.0 wt. % and dispersed ultrasonically for 180 min. The tribological behavior was evaluated on an MS-10J four-ball tester (Xiamen Tenkey Co. Ltd). The balls (12.7 mm in diameter) in the test were made of GCr15 bearing steel with a hardness of 59-61. The maximum nonseizure load (P_B) was determined according to the Chinese National Standard Method GB/T3142-90 (similar to ASTM D2738). Tests of the antiwear and friction reduction properties were conducted at 1200 rpm (20 s^{-1}) for 3600 s at room temperature at a load of 147 N. At the end of each test, the wear scar diameters (WSDs) of the three stationary balls were measured using an optical microscope to an accuracy of $\pm 0.01 \text{ mm}$ and the friction coefficients were recorded automatically with a strain gauge equipped with the four-ball tester.

Powder XRD patterns were recorded with an X-ray diffractometer (Rigaku, MiniFlex II) using $\text{CuK}\alpha$ radiation ($\lambda = 1.5418 \text{ \AA}$). The steel balls was cleaned with petroleum ether for 10 min in an ultrasonic bath before the SEM and EDS analysis. SEM micrographs were obtained for the powder samples (JEOL, JSM-6700E) and the worn surfaces (Hitachi, TM-3000). The chemical compositions of the surfaces of the friction pairs were analyzed by EDS (Bruker, QUANTAX 70). FT-IR spectra of the samples were obtained on a Shimadzu IRAffinity-1 FT-IR spectrometer using the KBr pellet technique.

RESULTS AND DISCUSSION

Microcrystals of ZIF-8 were synthesized by the solvothermal synthesis method and characterized by PXRD and

SEM. Fig. 1a shows the relative intensity and peak positions of the PXRD patterns, which are in agreement with the results of previous reports¹ and confirm the formation of pure crystalline ZIF-8. The SEM image in Fig. 1b shows that the microcrystalline product consists of relatively regular particles with a diameter distribution of 1-10 μm . The synthesis of nanocrystalline ZIF-8 was performed according to the reported method¹⁰. The PXRD patterns of the nanocrystalline ZIF-8 were the same (Fig. 1c) and the mean diameter was approximately 100 nm (Fig. 1d). The FT-IR spectrum of nano- and microcrystals of ZIF-8 are in good agreement with pure ZIF-8 prepared according to the literature (Fig. 2.)¹¹.

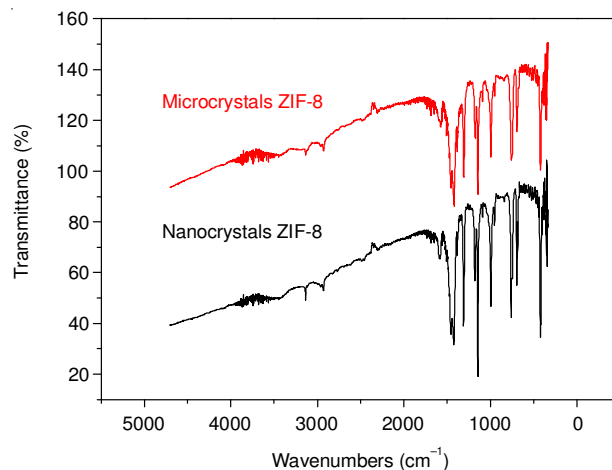


Fig. 2. FT-IR spectra of typical samples: nano- and microcrystals of ZIF-8

Friction and wear tests: Table-1 discloses the variation in the maximum nonseizure load (P_B) for the two additives as a function of the concentration of additives. It can be seen that the P_B value of the ZIF-8 microcrystals is improved by 17 % with additive concentrations ranging from 0.5 to 3.0 wt. % and that

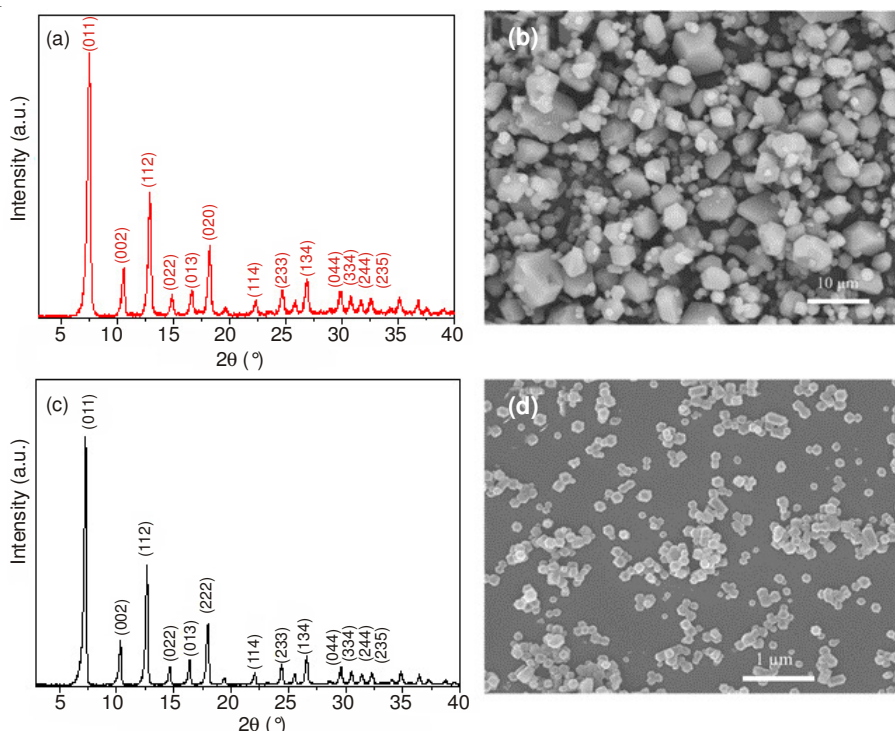


Fig. 1. PXRD patterns and SEM images of two particles sizes of ZIF-8: (a, b) microcrystals; (c, d) nanocrystals

Additive	PEG200	+0.5 wt. (%)	+1.0 wt. (%)	+2.0 wt. (%)	+3.0 wt. (%)
ZIF-8 (microcrystals)	510	598	598	598	598
ZIF-8 (nanocrystals)	510	549	549	549	549

of the nanocrystals is improved by 7.6 %. The microcrystals also show better load-carrying capacity than the nanocrystals.

Fig. 3 shows the variation of the wear scar diameters for the two additives as a function of the concentration of additives. The wear scar diameter (WSD) of nanocrystalline ZIF-8 is reduced from 0.52 mm (the WSD of pure PEG 200) to 0.36 mm at the additive concentration 0.5 wt.%. The WSD then increases somewhat from 0.38 to 0.39 mm when the additive concentration increases from 1.0 to 3.0 wt.%. Although the lowest WSD of the ZIF-8 microcrystals is also found at a concentration of 0.5 wt.% (0.36 mm), the WSD increase with additive concentrations ranging from 1.0 to 3.0 wt. % is greater than that of the nanocrystals, from 0.38 to 0.43 mm. Thus, the nanocrystalline ZIF-8 has better antiwear performance than the microcrystals.

And the nano- and microcrystals of ZIF-8 show no improvement in friction reduction property. Fig. 4. shows the relationship between the friction coefficient and the additive concentration. As additive, ZIF-8 nanocrystals is found to slightly reduce the friction coefficient from 0.097 to 0.091 with the concentration increasing from 0.5 to 1.0 wt. %, then increases gradually and reaches a plateau. With regard to microcrystals, the lowest friction coefficient is at 0.5 wt.% and higher than that of PEG 200 from 1.0 to 3.0 wt. %. The nano- and microcrystals of ZIF-8 show no improvement in friction reduction property.

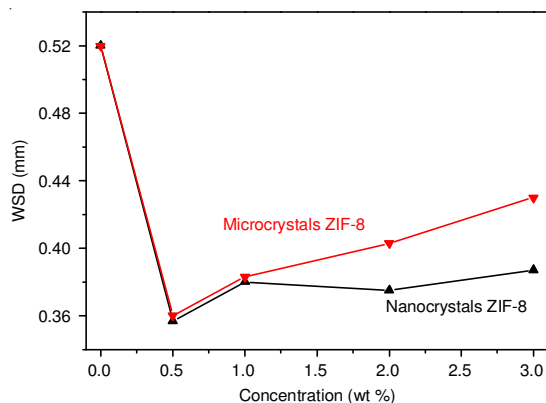


Fig. 3. Relationship between WSD of the lubricated balls and additive concentration (wt.%)

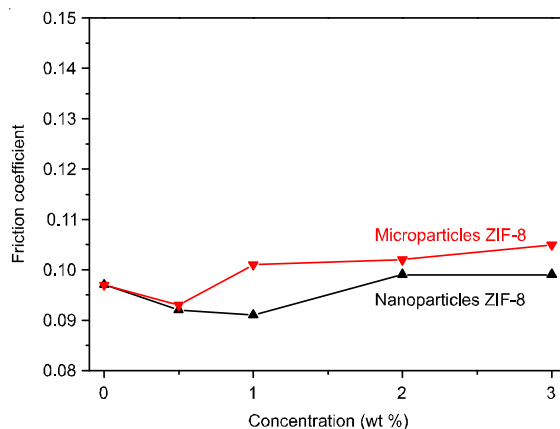


Fig. 4. Friction coefficient as a function of concentration

Fig. 5 presents the morphology and element composition of the worn surfaces of the friction pairs lubricated with PEG 200 containing 0.5 wt.% nano- or microcrystals. The wear scars of the steel balls containing 0.5 wt.% nano- or micro-

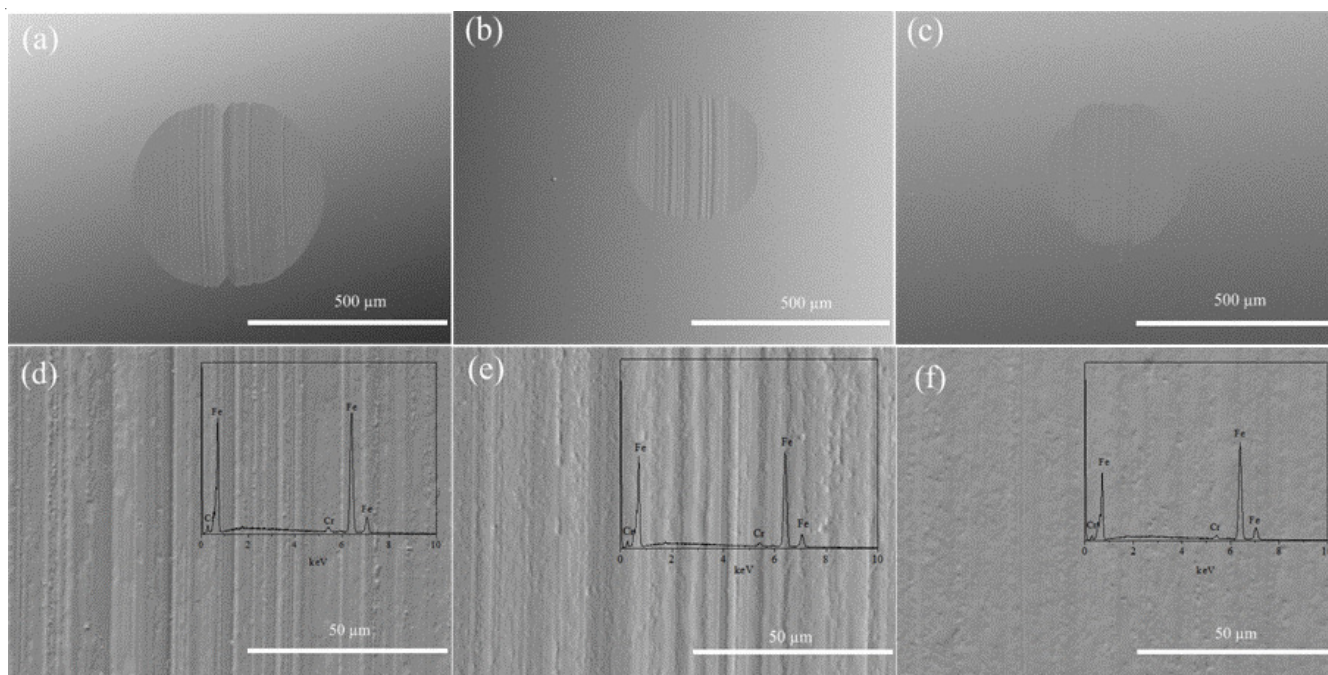


Fig. 5. SEM images and EDS of the worn surfaces of balls lubricated with a, d: pure PEG 200; b, e: 0.5 wt.% nanocrystalline ZIF-8; and c, f: 0.5 wt.% microcrystalline ZIF-8

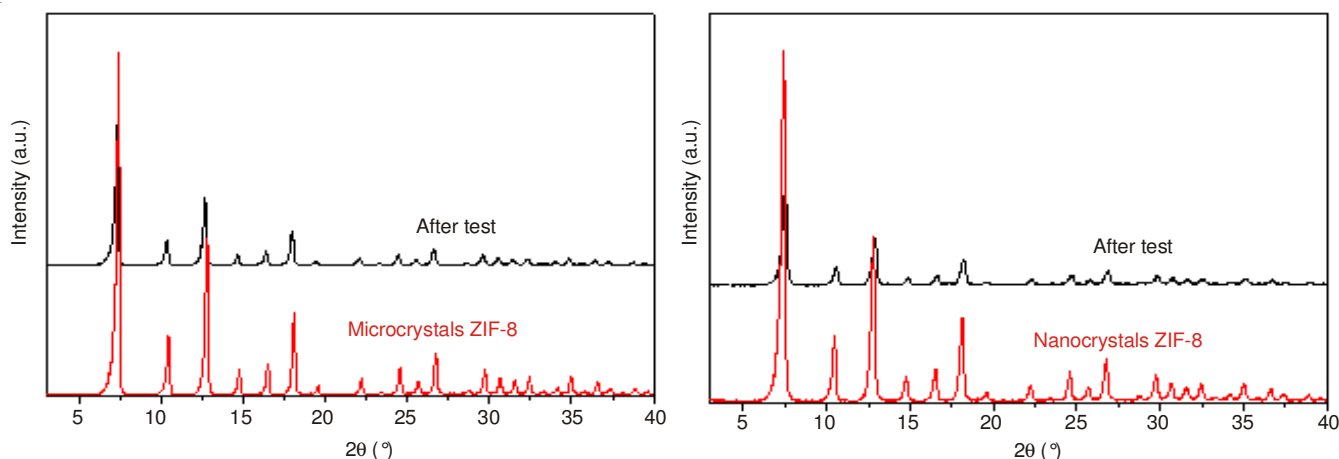


Fig. 6. XRD patterns of the ZIF-8 before and after antiwear test

crystals are much smoother and smaller than that of the steel ball lubricated with PEG 200 alone (Figs. 5a-c). The worn surface lubricated with PEG 200 alone is rough and shows signs of severe scuffing (Fig. 5d). However, scuffing on the surfaces lubricated with PEG 200 containing 0.5 wt.% nano- or microcrystals was significantly inhibited (Figs. 5e, f). Therefore, the results further testify that ZIF-8 nano- and microcrystals have good antiwear properties. The EDS spectra (Figs. 5d-f) show that no chemical elements other than steel components were detected on the wear surface after the antiwear test. The PXRD patterns of the nano- and microcrystals illustrate minimal changes in the diffraction peak positions before and after the lubricating test (Fig. 6).

Lubricating behaviour analysis: The lubricating behavior of ZIF-8 is linked to the intrinsic nature of a flexible 3D framework. Thus, the characteristic M-Im-M linkages in ZIF-8 are more compliant and can afford greater flexibility. For these reasons, the addition of nano- or microcrystals to the oil leads to an increase in the load capacity and excellent antiwear properties. Because the P_B test is a process with a very short run time (10 s), shearing is not extensive. Also, the larger particle size of the microcrystals had minimal impact on the framework distortion and thus microcrystals exhibited better load-carrying capacity than nanocrystals. However, when the antiwear test was run for 3600 s, the nanocrystals tended to deform and were quickly deposited on the rough metal surfaces, preventing direct contact between the two metal surfaces. This is the reason why nanocrystals have better antiwear performance than microcrystals.

Conclusion

ZIF-8 nano- and microcrystals exhibited good tribological behavior as additives in PEG200. The main wear mechanism

of ZIF-8 is the framework, which has low shear modulus and good structural stability. The low shear resistance of ZIF-8 reduced friction at the interfaces and microcrystalline ZIF-8 exhibited a better load-carrying capacity.

ACKNOWLEDGEMENTS

This work was financially supported by the National Natural Science Funds (Grant No. 51172153), the Natural Science Foundation of Shanxi Province (2011011022-3 and 2013021008-1).

REFERENCES

1. K.S. Park, Z. Ni, A.P. Côté, J.Y. Choi, R. Huang, F.J. Uribe-Romo, H.K. Chae, M. O'Keeffe and O.M. Yaghi, *Proc. Natl. Acad. Sci. USA*, **103**, 10186 (2006).
2. R. Banerjee, A. Phan, B. Wang, C. Knobler, H. Furukawa, M. O'Keeffe and O.M. Yaghi, *Science*, **319**, 939 (2008).
3. H. Bux, F. Liang, Y. Li, J. Cravillon, M. Wiebcke and J. Caro, *J. Am. Chem. Soc.*, **131**, 16000 (2009).
4. H.-L. Jiang, B. Liu, T. Akita, M. Haruta, H. Sakurai and Q. Xu, *J. Am. Chem. Soc.*, **131**, 11302 (2009).
5. J.-C. Tan, B. Civalieri, C.-C. Lin, L. Valenzano, R. Galvelis, P.-F. Chen, T.D. Bennett, C. Mellot-Draznieks, C.M. Zicovich-Wilson and A.K. Cheetham, *Phys. Rev. Lett.*, **108**, 095502 (2012).
6. Q. Shi, Z. Chen, Z. Song, J. Li and J. Dong, *Angew. Chem.*, **123**, 698 (2011).
7. S. Chen and W. Liu, *Mater. Chem. Phys.*, **98**, 183 (2006).
8. G. Sui, W. Zhong, X. Ren, X. Wang and X. Yang, *Mater. Chem. Phys.*, **115**, 404 (2009).
9. A. Hernández Battez, R. González, J. Viesca, J. Fernández, J. Díaz Fernández, A. Machado, R. Chou and J. Riba, *Wear*, **265**, 422 (2008).
10. J. Cravillon, S. Münzer, S.-J. Lohmeier, A. Feldhoff, K. Huber and M. Wiebcke, *Chem. Mater.*, **21**, 1410 (2009).
11. Y. Hu, H. Kazemian, S. Rohani, Y. Huang and Y. Song, *Chem. Commun.*, **47**, 12694 (2011).